Analytica Chimica Acta 1134 (2020) 96–105

Contents lists available at ScienceDirect

Analytica Chimica Acta

journal homepage: www.elsevier.com/locate/aca

Cu/Au/Pt trimetallic nanoparticles coated with DNA hydrogel as target-responsive and signal-amplification material for sensitive detection of microcystin-LR

Pian Wu [a, b, c], Shuang Li [b], Xiaosheng Ye [a, c], Baoan Ning [b], Jialei Bai [b], Yuan Peng [b], Lei Li [d], Tie Han [b], Huanying Zhou [b], Zhixian Gao [b, **], Ping Ding [a, c, *]

[a] Xiang Ya School of Public Health, Central South University, Changsha, Hunan, 410078, PR China
[b] Tianjin Key Laboratory of Risk Assessment and Control Technology for Environment and Food Safety, Tianjin Institute of Environment and Operational Medicine, Tianjin, 300050, PR China
[c] Hunan Provincial Key Laboratory of Clinical Epidemiology, Changsha, Hunan, 410078, PR China
[d] Center for Global Health, School of Public Health, Nanjing Medical University, Nanjing, 211166, PR China

HIGHLIGHTS

- A novel Cu/Au/Pt TNs-encapsulated DNA hydrogel with target-responsive and signal-amplification was prepared.
- A colorimetric platform based on this DNA hydrogel was established for sensitive detection of MC-LR.
- The colorimetric platform can detect MC-LR with a detection limit to 3.0 ng L^{-1}.
- This strategy can be applied to other targets by designing complementary strands of relative aptamer.

GRAPHICAL ABSTRACT

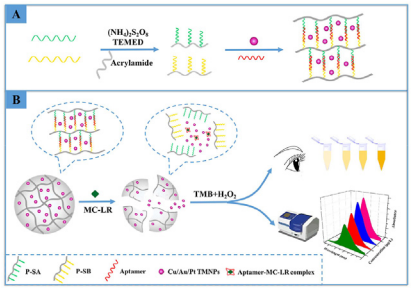

ARTICLE INFO

Article history:
Received 9 April 2020
Received in revised form
31 July 2020
Accepted 2 August 2020
Available online 13 August 2020

Keywords:
Cu/Au/Pt trimetallic nanoparticles
Microcystin-LR
DNA hydrogel
Signal amplification
Detection

ABSTRACT

Sensitive and reliable analytical methods for monitoring of microcystin-LR (MC-LR) are urgently necessary due to its great harm to human health and aquatic organisms. In this work, a novel Cu/Au/Pt trimetallic nanoparticles (Cu/Au/Pt TNs)-encapsulated DNA hydrogel was prepared for colorimetric detection of MC-LR. The Cu/Au/Pt TNs were captured and released with precise control by the target-responsive 3D DNA hydrogels, which combined dual advantages of the target responsive DNA hydrogel and Cu/Au/Pt TNs of enhanced peroxidase-like activity. The DNA hydrogel network was constructed by hybridizing MC-LR aptamer with two complementary DNA strands on linear polyacrylamide chains. As long as MC-LR presented, the aptamer competitively binds with the MC-LR, causing the hydrogel to dissolve and release the preloaded Cu/Au/Pt TNs which could catalyze the reaction between H_2O_2 and TMB to produce color changes. In view of this sensitive strategy, this Cu/Au/Pt TNs-encapsulated DNA hydrogel-based colorimetric biosensor can achieve quantitative determination of MC-LR. The results showed that as-proposed colorimetric biosensor could sensitively detect MC-LR with a linear range of 4.0 −10000 ng L^{-1} and a detection limit of 3.0 ng L^{-1}. This work proved that the sensor had great potential to

* Corresponding author. Xiang Ya School of Public Health, Central South University, Changsha, Hunan, 410078, PR China.
** Corresponding author.
E-mail addresses: gaozhx@163.com (Z. Gao), pingshui@csu.edu.cn (P. Ding).

https://doi.org/10.1016/j.aca.2020.08.004

be applied in MC-LR detection and also provided the opportunity to develop colorimetric biosensor for other targets using this target-responsive and signal-amplification strategy.

1. Introduction

In recent years, a large number of biologically active microcystins (MCs) are released into the environment due to the frequent occurrence of cyanobacteria blooms, which bring a tremendous threat to human health and aquatic organisms [1,2]. Microcystin-LR (MC-LR) is the most widely distributed and most toxic homologues among kinds of microcystin congeners [3]. It has been reported that MC-LR is directly correlated with tumor promotion and can lead to the occurrence of liver cancer even in the case of chronic low-level exposure [4]. The World Health Organization (WHO) recommends that the concentration of MC-LR in drinking water does not exceed 1.0 μg L^{-1} [5]. Thus, a precise, sensitive and reliable analytical method for monitoring of MC-LR is urgently necessary for the purpose of protecting environmental safety and ensuring human health.

Lots of laboratory approaches for MC-LR detection have been reported, covering high performance liquid chromatography (HPLC) [6], enzyme-linked immunosorbent assay (ELISA) [7] and liquid chromatography tandem mass spectrometry (LC-MS) [8]. Despite the sensitivity and accuracy these approaches have, most of them require sophisticated operation procedures and complicated instruments. Recently developed chemical sensors and biosensors are considered to be promising analytical techniques. Biosensors based on fluorescence, electrochemistry, raman, chemiluminescence and colorimetry have been well-developed with high selectivity and sensitivity [9–13].

Among various biosensors, colorimetric-based sensors could be ideal for target detection because colorimetric sensors can output the signal with a simple portable spectrometer, or image processing software, even distinguished with naked eye [14,15]. However, the sensitivity of conventional colorimetric methods is usually not unsatisfactory [13,16]. In order to solve this problem, amplification strategies such as enzymes and bio-active nanomaterials are usually introduced when constructing colorimetric sensors [17,18]. Nevertheless, natural enzymes such as horseradish peroxidase (HRP) and glucose oxidase (GOD) could be easily affected by the environment during using. So, the nanocomposites to mimic natural enzymes have been developed rapidly in recent decades [19,20]. In our previous study, we have fabricated a novel Cu/Au/Pt trimetallic nanoparticle (Cu/Au/Pt TN) which possesses stronger catalytic activity than monometallic or bimetallic nanoparticle, and we have successfully demonstrated its promising application in colorimetric sensors for H_2O_2, glucose and cancer cell biosensing [21,22]. These prepared Cu/Au/Pt TNs have multiple advantages of good stability, sustainable catalytic activity, robustness to harsh environments and facile ligand conjugation, which facilitate the development of Cu/Au/Pt TNs in the applications of biosensing. On the basis of the catalytic effect of Cu/Au/Pt TNs on the reaction between 3,3,5,5-tetramethylbenzidine (TMB) with hydrogen peroxide (H_2O_2), a colorimetric detection strategy could also be established for MC-LR detection.

The key to fabricate Cu/Au/Pt TNs-based colorimetric biosensor is that the color signal produces from Cu/Au/Pt TNs catalysis changes following the target concentration. Since Nagahara first reported the DNA-polymer hybrid hydrogel in 1996 [23], DNA hydrogels have drawn wide research attention because of their great potential in biomedical and biosensing applications, such as the detection of ATP [24,25], cocaine [26,27], miRNA [28,29] and mycotoxins [30,31]. DNA hydrogels are 3D crosslinked networks which can encapsulate enzymes and nanomaterials. Target-responsive hydrogels can be constructed by designing responsive polymeric backbones or responsive crosslinking units as a switch which could be turned "ON" or "OFF" with or without its target [32]. When the switch is opened by the target, those encapsulated enzymes and nanomaterials will be released as signal output.

Inspired by the pioneering works above, DNA hydrogels encapsulated with Cu/Au/Pt TNs were prepared as target-responsive and signal-amplification materials to fabricate a novel sensing platform for the sensitive detection of MC-LR. In this newly designed sensor, a MC-LR specific aptamer was incorporated into hydrogels as responsive cross-linkers, the Cu/Au/Pt TNs were encapsulated into hydrogels as signal amplification and output units. Such strategy shows an integration of DNA hybridization and nanoparticle-mediated catalysis and exhibits excellent performance in the quantitative assay of MC-LR for food safety and water quality.

2. Experimental section

2.1. Materials and reagents

30% H_2O_2, $HAuCl_4 \cdot H_2O$ (>99.5%), $CuSO_4 \cdot 5H_2O$, $NaBH_4$, Sodium citrate, N,N,N′,N′-tetramethylethylenediamine (TEMED), Ammonium persulfate (APS) and Acrylamide were obtained from Damao chemical reagent factory (Tianjin, China). K_2PtCl_4 (>99.9%), 3,3,5,5-tetramethylbenzidine (TMB), chloramphenicol (CH) and estradiol (E2) were obtained from Sigma-Aldrich (St.Louis, MO, USA). Microcystin-LR (MC-LR) and Microcystin-RR (MC-RR) were purchased from Algalchem Inc. (Taiwan, China). Microcystin-YR (MC-YR) was obtained from Abraxis Inc. (Warminster, PA, USA). All oligonucleotides applied in this work were synthesized and modified by Shanghai Sangon Biotechnology Co., Ltd. (Shanghai, China) and purified by high performance liquid chromatography (HPLC). The sequences of these oligonucleotides were as follows:

Strands-A (SA): 5′-Acrydite-TTT TTT **GGG CAT AAT GAG**-3'.

Strands-B (SB): 5′-Acrydite-TTT TTT GTA ATT GTC ATG-3'.

MC-LR aptamer: 5′-GGC GCC AAA CAG GAC CAC CAT GAC AAT TAC CCA TAC CAC **CTC ATT ATG CCC** CAT CTC CGC-3'.

2.2. Apparatus

The colorimetric determination were performed by UV–Vis spectrophotometer (TU-1901, Persee Co., Ltd., China). Transmission electron microscopy (TEM, FEI talos F200X, USA) and scanning electron microscope (SEM, VEG3 TESCAN, Czech Republic) were employed to characterize the resulting nanocomposites. Circular dichroism (CD, J-715, JASCO, Japan) was used to analyze changes in DNA conformation. The electrophoresis apparatus (DYY-11, Liuyi Instrument Factory, China) and ImageQuant 350 gel imaging system (GE Healthcare, USA) were also used in experiments.

2.3. Synthesis of Cu/Au/Pt TNs-DNA hydrogels

Prior to preparation of Cu/Au/Pt TNs-encapsulated DNA hydrogel, the Cu/Au/Pt TNs were synthesized according reported methods [21,22]. Briefly, $CuSO_4$, sodium citrate and $NaBH_4$ were added into water under rapid mixing with a final concentrations of 0.12 mmol L^{-1}, 0.25 mmol L^{-1} and 1.25 mmol L^{-1} respectively. About 15 min later, $HAuCl_4$ and K_2PtCl_4 were added with the final concentrations of 0.25 mmol L^{-1} and stirring was continued for about 20 min. The synthesized Cu/Au/Pt TNs were stored at room temperature for further application.

The Cu/Au/Pt TNs-DNA hydrogels were prepared based on the reported procedures with some modification [31]. Firstly, the DNA side-chain polymer was synthesized through the following procedure: 30 μL acrydite-DNA solution (SA or SB, 300 μmol L^{-1}), 7.8 μL PBS, and 14.4 μL acrylamide (25 wt%) were mixed vigorously and kept under vacuum for 10 min to remove the air. Followed by adding 12.6 μL APS (10 wt%) and 25.2 μL TEMED (5 wt%). Then, the mixture was immediately incubated under vacuum for 15 min to obtain the polymer strands. Secondly, the Cu/Au/Pt TNs-encapsulated DNA hydrogels were prepared as follows: the 2 μL P-SA (100 μmol L^{-1}), 2 μL P-SB (100 μmol L^{-1}), 4 μL Cu/Au/Pt TNs prepared above, and 2 μL MC-LR aptamer (35 μmol L^{-1}) were mixed in the eppendorf tube. Subsequently, the mixed solution was incubated twice at 65 °C for 5 min and was shaken vigorously after each incubation. Finally, the mixture was cooled to room temperature to form the Cu/Au/Pt TNs-encapsulated DNA hydrogels.

2.4. Native polyacrylamide gel electrophoresis

In order to verify the cross-linking effect of aptamer to SA and SB as well as the binding ability of aptamer to MC-LR, SA, SB, aptamer and the mixture of aptamer/SA/SB in PBS buffer were heated to 95 °C for 5 min and slowly cooled to 25 °C. Subsequently, the different concentrations MC-LR were added in the mixture of aptamer/SA/SB and incubated at 25 °C for 40 min. A 12% native polyacrylamide gel electrophoresis (PAGE) was prepared with 1 × TBE buffer (90 mM Tris-HCl, 2 mM EDTA, 90 mM boric acid, pH 7.8). Then the gel was run at 100 V for 70 min and stained with gene green for 30 min. The photo was taken by the ImageQuant system.

2.5. Assay procedure

MC-LR (10 μL) with different concentrations were added to that prepared hydrogels, followed by incubation at 25 °C for 40 min to ensure the complete competitive reaction between complementary DNA and MC-LR. Then 198 μL H_2O, 12 μL TMB (333 μmol L^{-1}) and 12 μL H_2O_2 (1.0 mol L^{-1}) were added sequencely for catalytic reaction. After incubating at room temperature for about 10 min, the reaction was terminated by 1 mol L^{-1} HCl, and the absorbance was determined by UV–Vis spectrometer at 452 nm immediately.

2.6. Analysis of MC-LR in actual samples

For the detection of MC-LR in real samples, fresh crucian carp tissue purchased from supermarket and tap water taken from Tianjin Water Group were selected to assess the accuracy the proposed assay. Various accounts of MC-LR standards were spiked into fresh fish tissue and water samples with the final concentrations of 100 and 1000 ng L^{-1}, respectively. Then the spiked samples were determined by the above-described procedure and microcystin ELISA kit at the same time.

3. Results and discussion

3.1. Working principle of the proposed biosensor

The design of MC-LR-responsive hydrogel was displayed in Scheme 1. Strands-A and strands-B were designed to be complementary to two adjacent regions of the MC-LR aptamer and were grafted onto linear polyacrylamide polymers to form polymer strands A and B (P-SA and P-SB). MC-LR aptamers act as cross-linkers were used to hybridize with SA and SB to form hydrogels. Cu/Au/Pt TNs were encapsulated in DNA hydrogels. When in presence of MC-LR, the specific aptamers competitively binded with the MC-LR and form target-aptamer complexes due to high affinity between aptamer and target, causing the disintegration of hydrogels and the release of preloaded Cu/Au/Pt TNs. Cu/Au/Pt TNs with enhanced enzymes activity would catalyze the reaction between H_2O_2 and TMB, producing color changes as the concentration of MC-LR changes.

3.2. Feasibility verification

The design of the complementary DNA strands is very important for the construction of hydrogels. In order to prove the cross-linking effect of aptamer to SA and SB as well as the binding ability of aptamer to MC-LR, the hybridization and dehybridization performance of the three complementary DNA strands were studied by circular dichroism and native-PAGE. As exihibited in Fig. 1A, MC-LR showed no peaks of secondary structures. The mixture of SA and SB showed similar peaks to the aptamer which displayed a positive peak at about 280 nm and a negative peak at about 245 nm. When the SA and SB was added into the aptamer solution, there were slight red shift at 280 nm and slight blue shift at 248 nm, and the peaks were significantly decrease, indicated that their secondary structure changed due to the hybridization of aptamer, SA and SB. However, there was a strong increase at 280 nm and 245 nm after introducing MC-LR into the mixture of aptamer, SA and SB, indicated that MC-LR could successfully compete for the aptamer from the complementary DNA strands. These results were further supported by the results of native-PAGE in Fig. 1B, which demonstrated that the existence of MC-LR induced a disruption of the three complementary DNA strands. Taken together, MC-LR aptamer can efficiently hybridize with SA and SB to form a triple-stranded complex. Equally important is that the triple-stranded complex could be efficiently dehybridizated in the presence of MC-LR.

In order to validate the feasibility of Cu/Au/Pt TNs-encapsulated DNA hydrogel biosensor, a simple control experiment was performed. As shown in Fig. 2, in the absence of aptamer, a high absorbance value was observed whether or not MC-LR was presented, indicating that Cu/Au/Pt TNs were not successfully encapsulated (line a and b). When the aptamer was added, the lowest absorbance intensity was obtained due to the formation of hydrogels by the addition of aptamer (line c). If we added MC-LR on this basis, the absorbance value of the system increased significantly because the combination between aptamer and MC-LR was occurred and the hydrogels were further disrupted (line d). Fig. S1 further confirm the feasibility of Cu/Au/Pt TNs-encapsulated DNA hydrogel biosensor because the absorbance value of the system increased significantly and the color of the solution changed from colorless to yellow in the presence of MC-LR, while no evident changes occured in absence of MC-LR.

3.3. Characterization

To prove that the Cu/Au/Pt TNs were successfully synthesized, TEM was performed, and the results were showed in Fig. 3. The

synthesized Cu/Au/Pt TNs had a spheroidal structure (Fig. 3A). It can also be observed that the Cu, Au and Pt elements were distributed evenly in Cu/Au/Pt TNs (Fig. 3B–F). The TEM and SEM were also applied to characterize the formation of DNA hydrogels. A typical three-dimensional network structure was observed and the Cu/Au/Pt TNs were embedded in DNA hydrogel (Fig. 4). These results suggested that the Cu/Au/Pt TNs-encapsulated DNA hydrogels were successfully synthesized.

3.4. Optimization of experimental conditions

Some experimental conditions which affected the performance of the proposed sensor were optimized. To prepare stable and sensitive hydrogels, the concentrations of aptamer-linker were firstly optimized. As shown in Fig. 5A–D, the dissociation kinetics in the presence of different MC-LR concentrations were observed by monitoring the absorbance value at 452 nm, which is the absorption maximum for oxidized TMB. When 30 μmol L^{-1} aptamer-linker was used, high absorbance value was obtained after MC-LR added. However, the absorbance increased significantly as time increased even no MC-LR added, which indicated the weak stability of the hydrogels (Fig. 5A). When the aptamer concentration was 35 μmol L^{-1}, the absorbance increased significantly with the addition of MC-LR and the absorbance had little change without MC-LR, indicating that hydrogels were stable and sensitive (Fig. 5B). When the aptamer concentrations were higher than 35 μmol L^{-1}, there was a little change of absorbance value with MC-LR addition which meaned that high sensitivity would not be achieved under this condition (Fig. 5C–D). Hence, 35 μmol L^{-1} aptamer was selected as the optimum concentration to synthesize stable DNA hydrogel with ideal sensitivity to MC-LR. It could also be seen from Fig. 5B that the absorbance value of the MC-LR-containing group remained almost unchanged after 40 min incubation, indicating that 40 min of incubation was enough for the combination of MC-LR with aptamer. Thus, the optimum incubation time was 40 min.

It is also important to optimize the amount of Cu/Au/Pt TNs encapsulated in the hydrogels because they would significantly affect the sensitivity of the assay. Fig. 5E exihibited the effects of the amount of encapsulated Cu/Au/Pt TNs on the changes in absorbance. The highest absorbance change could be obtained as the volume of the encapsulated Cu/Au/Pt TNs was 4.0 μL. It was because the lower amount of Cu/Au/Pt TNs encapsulated resulting in smaller signal change, while the higher amount of Cu/Au/Pt TNs overloaded resulting in higher background signal. The concentrations of H_2O_2 and TMB were also optimized. Since the Cu/Au/Pt TNs released from DNA hydrogel partly depended on the amount of MC-LR, 4.0 μL Cu/Au/Pt TNs, the maximum amount of encapsulation in the hydrogel, was used to explore the optimal H_2O_2 and TMB concentrations. As shown in Fig. S2 and Fig. S3, it is enough for Cu/Au/Pt TNs to achieve their maximum catalytic efficiency when the concentrations of H_2O_2 and TMB are 48 mmol L^{-1} and 26.4 mmol L^{-1}, respectively. Moreover, pH could effect the catalytic activity of Cu/Au/Pt TNs, it could be seen from Fig. S4 that the optimal pH was 5.

3.5. Colorimetric response of the assay

To demonstrate the ability of the presented sensing approach to sensitive quantitation of MC-LR, colorimetric analysis was conducted under different concentrations of MC-LR. Fig. 6A showed positive correlations between the absorbance and the concentrations of MC-LR, the absorbance value enhanced as the MC-LR concentration increased. It could be seen from Fig. 6B that the absorption value was linearly related to the concentration of MC-LR in the range of 4.0–10000 ng L^{-1}, and the linear equation was $\triangle A = 0.0878 \lg C_{MC\text{-}LR} + 0.2519$ ($R^2 = 0.9911$). The limit of detection (LOD) of 3.0 ng L^{-1} was obtained from interpolating the mean value plus three standard deviations of blank samples (n = 11). Compared to the previously reported method, this Cu/Au/Pt TNs-DNA hydrogel based colorimetric biosensor exihibited better analytical performance (Table 1).

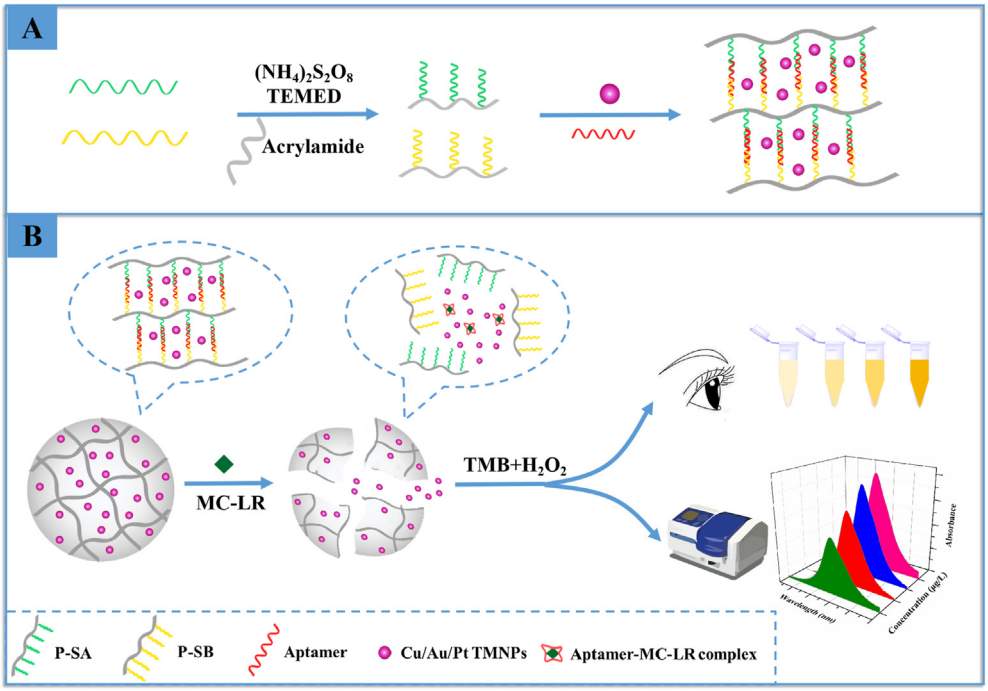

Scheme 1. Schematic illustration of the colorimetric biosensor for the detection of MC-LR based on the Cu/Au/Pt TNs-encapsulated DNA hydrogel.

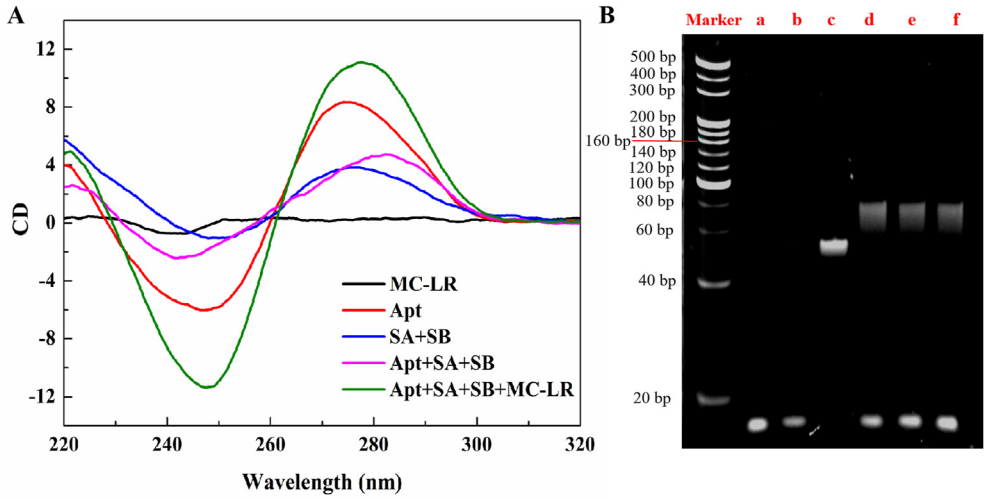

Fig. 1. (A) CD spectra of the oligonucleotides used in DNA hydrogel; The concentrations of all DNA were 10 μmol L^{-1} and the concentration of MC-LR was 10 μg L^{-1}. (B) Native-PAGE image of the oligonucleotides used in DNA hydrogel; a: SA; b: SB; c: aptamer; d: aptamer + SA + SB; e: aptamer + SA + SB + MC-LR (12.5 μg L^{-1}); f: aptamer + SA + SB + MC-LR (125 μg L^{-1}); The concentrations of SA, SB and aptamer were 2.0 μmol L^{-1}, 2.0 μmol L^{-1} and 1.0 μmol L^{-1}, respectively.

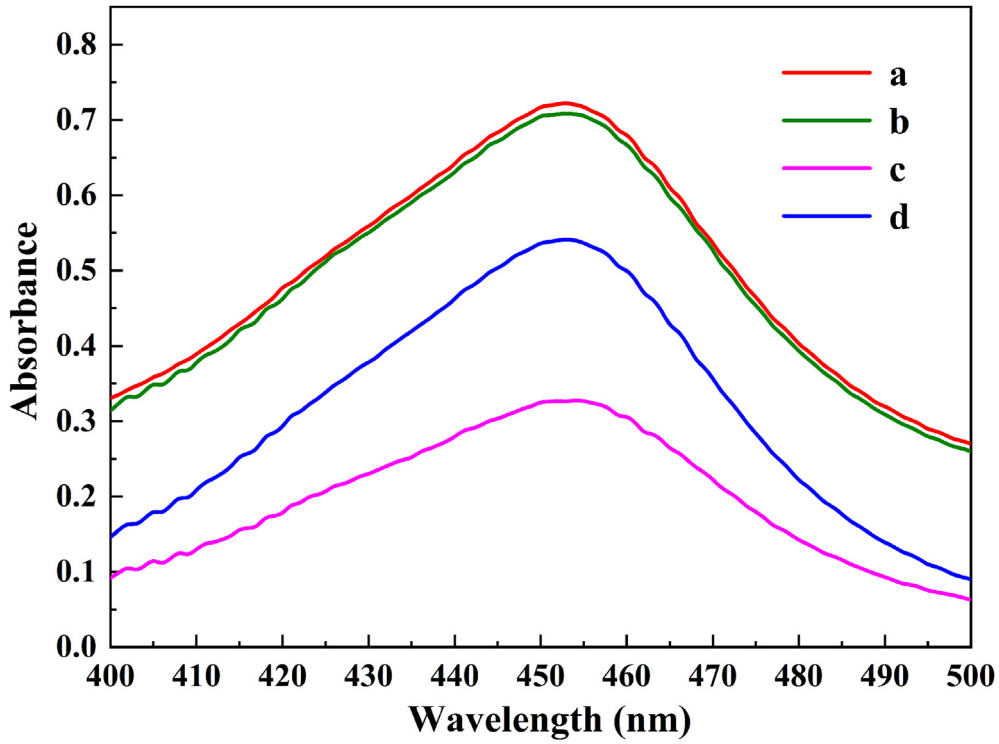

Fig. 2. UV–visible absorption spectra of the colorimetric biosensor under different conditions. (line a: no aptamers and no MC-LR added, line b: no aptamers but MC-LR added, line c: no MC-LR but aptamers added, line d: aptamers and MC-LR were added).

3.6. The specificity of the biosensor

To check the selectivity of the proposed method, two structure analogues (MC-RR and MC-YR) from the family of microcystins and two common small molecule contaminants (E2 and CH) in food and the environment were studied by measuring its relative absorbance with the same experimental method to MC-LR. As displayed in Fig. 7, only MC-LR caused a significant change of absorbance signal and other interferences produced little change in absorbance even the concentrations of these interferences were 10-flod higher (10.0 μg L^{-1}) than that of MC-LR (1.0 μg L^{-1}), demonstrating high specificity of the developed strategy for the determination of MC-LR.

3.7. Application of the biosensor

The reliability and feasibility of the as-proposed biosensor for quantifying MC-LR in actual samples were assessed by analyzing MC-LR in fresh crucian carp tissue and water spiked with a range of known concentrations of MC-LR. Table 2 showed the recoveries of fresh fish tissue and water sample, the recoveries of fresh crucian carp tissue were in the range of 95.34%–107.07% with relative

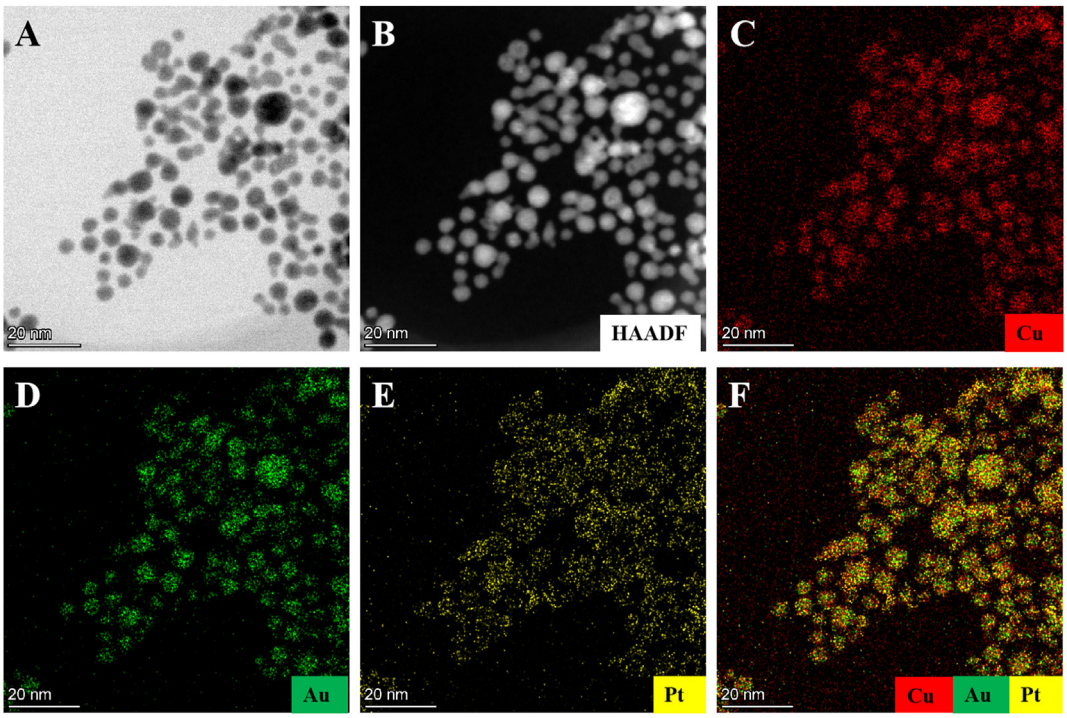

Fig. 3. Characterization of Cu/Au/Pt TNs. (A) TEM image of Cu/Au/Pt TNs. (B) STEM image of Cu/Au/Pt TNs. (C–E) STEM-EDS elemental mapping images of (C) Cu, (D) Au, and (E) Pt of Cu/Au/Pt TNs. (F) The merged image of C, D, and E.

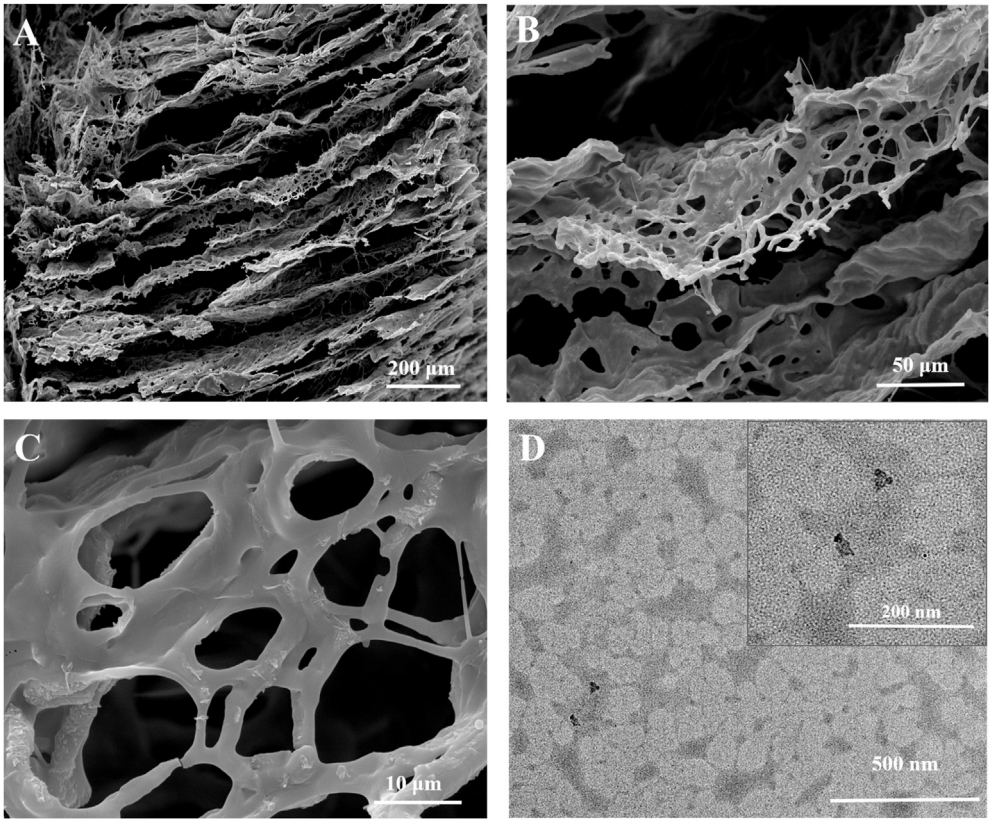

Fig. 4. Characterization of DNA hydrogels. (A–C) SEM images of DNA hydrogel. (D) TEM image of DNA hydrogel.

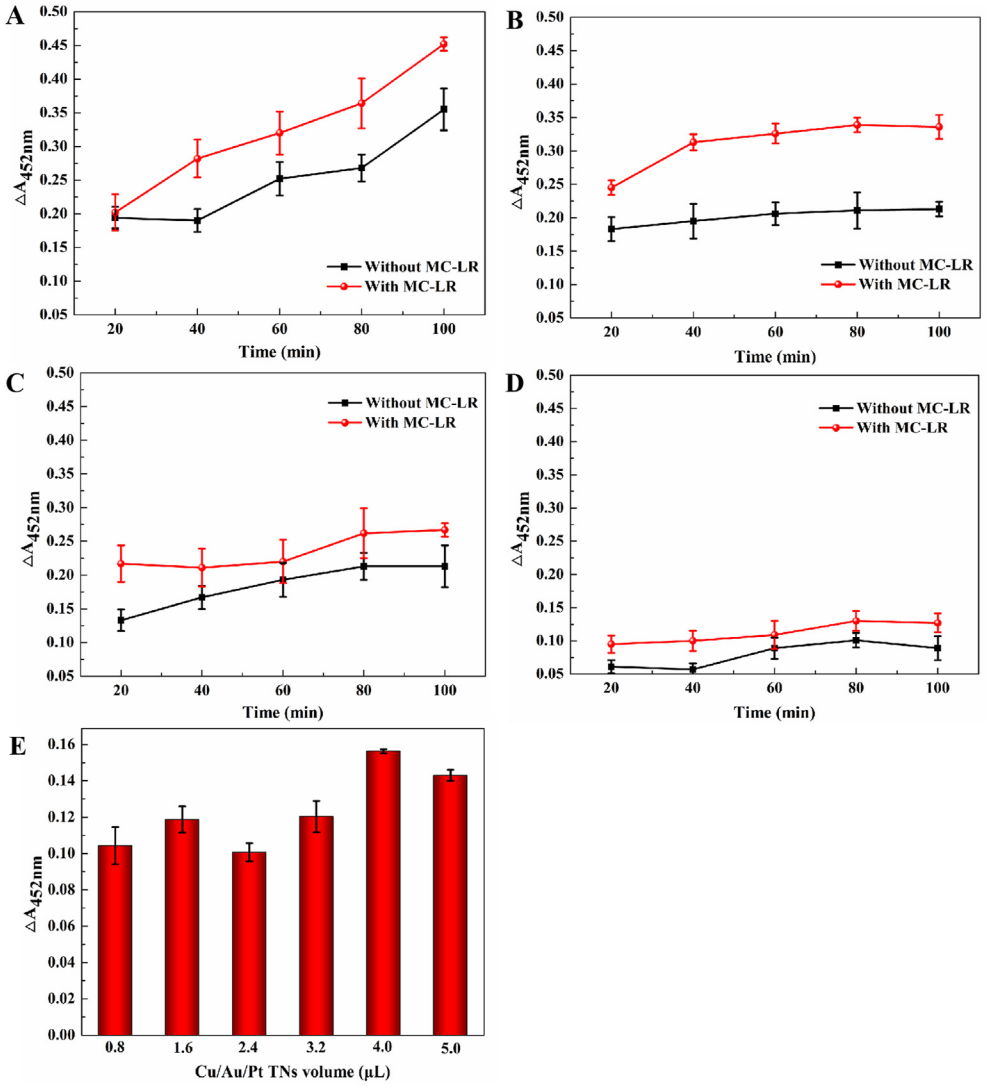

Fig. 5. (A–D) Effects of aptamer concentrations on Cu/Au/Pt TNs-encapsulated DNA hydrogel; Kinetics of hydrogel decomposition monitored at 452 nm when (A) 30 μmol L^{-1}, (B) 35 μmol L^{-1}, 40 μmol L^{-1} and (D) 50 μmol L^{-1} aptamer were used. (E) Effects of the Cu/Au/Pt TNs volume on the performance of the hydrogel.

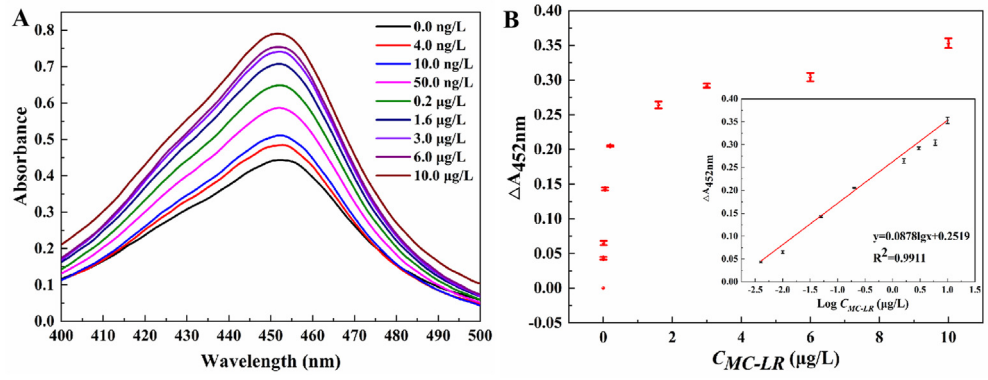

Fig. 6. (A) UV–visible absorption spectra of the Cu/Au/Pt TNs-encapsulated DNA hydrogel biosensor in the presence of various concentrations of MC-LR (0.0–10.0 μg L^{-1}). (B) Linear correlation between the changed absorption signal intensities and the concentrations of MC-LR.

standard deviations (RSDs) lower than 5.52%, while the recoveries of water ranged from 93.96% to 105.33% and the RSDs were less than 12.01%. The results were compared with the commercial ELISA kit, the recoveries obtained from the ELISA kit were 90.58%–108.82% (fresh crucian carp tissue) and 89.55%–102.12% (water), respectively. These results showed that there is a good consistency

Table 1
Comparison of different analytical methods for MC-LR.

Methods	Technique	Linear range ($\mu g\ L^{-1}$)	LOD ($ng\ L^{-1}$)	Ref.
Eu nanospheres	Fluorescence	0.1–5.0	54.2	[9]
SWCNTs-dapoxyl	Fluorescence	0.4–1194	137.0	[33]
QD-hapten nanoprobes	Fluorescence	0.10-4.0	30.0	[34]
Antibody-antigen	Chemiluminescence	0.062-0.65	30.0	[12]
Terminal deoxynucleotidyl transferase	Electrochemical	0.0597–995.189	14.9	[10]
Au NPs@MIL-101	Electrochemical	0.05–75	20.0	[35]
AuNRs/MoS_2/Au	Electrochemical	0.01–20	5.0	[36]
3D graphene	Electrochemical	0.05–20	40.0	[37]
Molecularly-imprinted polymers and AuNPs	Colorimetry	0.1–100	40.0	[13]
AuNPs	Colorimetry	0.5–7500	368.2	[16]
AuNP dimers	Colorimetry	0.1–250	49.6	[38]
Cu/Au/Pt TNs-encapsulated DNA hydrogel	Colorimetry	0.004–10	3.0	This work

Abbreviations: single-walled carbon nanotubes (SWCNTs), quantum-dot (QD), a composite material which Au nanoparticles were loaded on MIL-101 (Au NPs@MIL-101), gold nanorods/molybdenum disulfide/gold electrode (AuNRs/MoS_2/Au), Au nanoparticles (Au NPs).

between the results obtained from the presented biosensor and ELISA kit, indicated the potential application of that Cu/Au/Pt TNs-encapsulated DNA hydrogel biosensor for MC-LR detection.

4. Conclusion

In summary, a novel Cu/Au/Pt TNs-encapsulated DNA hydrogel was prepared and a colorimetric platform based on this DNA hydrogel was established for sensitive detection of hazardous MC-LR, which also confirms that the target-responsive and signal-amplification strategy are very effective and can be used for the measurement of other targets. Introduction of DNA hydrogel in the sensing system can solve the problem of detection specificity, and the introduction of Cu/Au/Pt TNs with intensive peroxidase-like activity can solve the problem of detection sensitivity, and visible color changes is more conducive to practical applications. Such strategy combines the advantages of the simple, available, and portable colorimetric system with superior performance of DNA hydrogel-based switchable release system, as well as the high target specificity of aptamer and robust properties of multimetallic

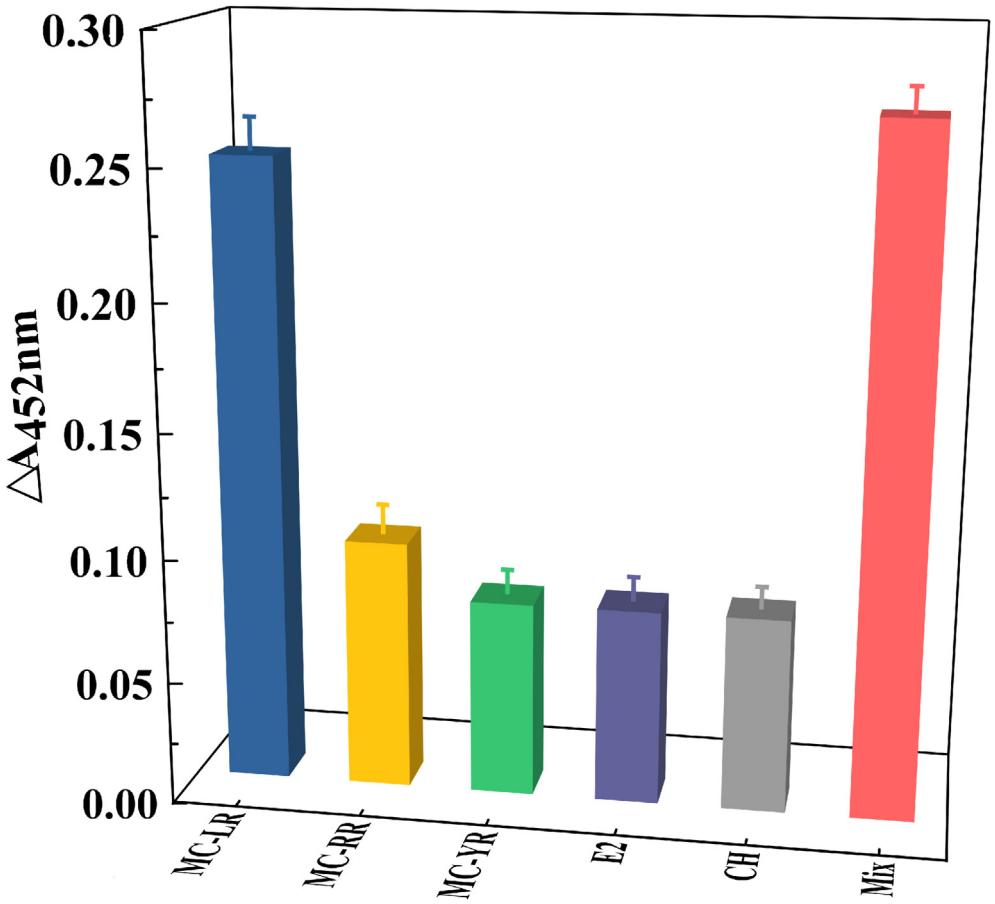

Fig. 7. Selectivity of the Cu/Au/Pt TNs-encapsulated DNA hydrogel biosensor; The concentration of MC-LR were 1.0 $\mu g\ L^{-1}$ and the concentrations of MC-RR, MC-YR, E2 and CH were all 10 $\mu g\ L^{-1}$.

Table 2
Determined results of MC-LR in real samples using the developed sensor and the ELISA Kit (n = 3).

Sample	Added (ng L^{-1})	Developed sensor			ELISA Kit		
		Detected (μg L^{-1})	Recovery (%)	RSD (%)	Detected (μg/L)	Recovery (%)	RSD (%)
Fish	0	ND#	–	–	ND#	–	–
	100	107.07	107.07	5.52	108.82	108.82	8.28
	1000	953.36	95.34	7.86	905.78	90.58	3.10
Water	0	ND	–	–	ND	–	–
	100	105.33	105.33	7.86	102.12	102.12	16.08
	1000	939.60	93.96	12.01	895.45	89.55	3.48

Not detected.

nanoparticles. In view of these advantages, this colorimetric biosensor achieved the detection limit of 3.0 ng L^{-1} and the detection range from 4.0 to 10000 ng L^{-1} which provide potential for analysis in actual samples.

CRediT authorship contribution statement

Pian Wu: Conceptualization, Writing - original draft, Writing - review & editing. **Shuang Li:** Funding acquisition. **Xiaosheng Ye:** Resources. **Baoan Ning:** Data curation. **Jialei Bai:** Software. **Yuan Peng:** Data curation. **Lei Li:** Visualization. **Tie Han:** Investigation. **Huanying Zhou:** Formal analysis. **Zhixian Gao:** Supervision, Project administration. **Ping Ding:** Supervision, Writing - review & editing.

Declaration of competing interest

The authors declare that they have no known competing financial interests or personal relationships that could have appeared to influence the work reported in this paper.

Acknowledgements

This work was supported by the National Key R&D Program of China (grant numbers 2018YFC1603500, 2017YFC1601101) and National Natural Science Foundation of China (grant number 21676305).

Appendix A. Supplementary data

Supplementary data to this article can be found online at https://doi.org/10.1016/j.aca.2020.08.004.

References

[1] X. He, A. Wang, P. Wu, S. Tang, Y. Zhang, L. Li, P. Ding, Photocatalytic degradation of microcystin-LR by modified TiO_2 photocatalysis: a review, Sci. Total Environ. 743 (2020) 140694.
[2] T. Gorham, Y. Jia, C.K. Shum, J. Lee, Ten-year survey of cyanobacterial blooms in Ohio's waterbodies using satellite remote sensing, Harmful Algae 66 (2017) 13–19.
[3] Y. He, P. Wu, G. Li, L. Li, J. Yi, S. Wang, S. Lu, P. Ding, C. Chen, H. Pan, Optimization on preparation of Fe_3O_4/chitosan as potential matrix material for the removal of microcystin-LR and its evaluation of adsorption properties, Int. J. Biol. Macromol. 156 (2020) 1574–1583.
[4] C. Zheng, H. Zeng, H. Lin, J. Wang, X. Feng, Z. Qiu, J.A. Chen, J. Luo, Y. Luo, Y. Huang, L. Wang, W. Liu, Y. Tan, A. Xu, Y. Yao, W. Shu, Serum microcystin levels positively linked with risk of hepatocellular carcinoma: a case-control study in southwest China, Hepatology 66 (2017) 1519–1528.
[5] P. Wu, G. Li, Y. He, D. Luo, L. Li, J. Guo, P. Ding, F. Yang, High-efficient and sustainable biodegradation of microcystin-LR using Sphingopyxis sp. YF1 immobilized Fe_3O_4@chitosan, Colloids Surf., B 185 (2020) 110633.
[6] H. Thuret-Benoist, V. Pallier, G. Feuillade-Cathalifaud, Quantification of microcystins in natural waters by HPLC-UV after a pre-concentration step: validation of the analytical performances and study of the interferences, Environ. Toxicol. Pharmacol. 72 (2019) 103223.
[7] L. Reverté, D. Garibo, C. Flores, J. Diogène, J. Caixach, M. Campàs, Magnetic particle-based enzyme assays and immunoassays for microcystins: from colorimetric to electrochemical detection, Environ. Sci. Technol. 47 (2013) 471–478.
[8] A. Zastepa, F.R. Pick, J.M. Blais, A. Saleem, Analysis of intracellular and extracellular microcystin variants in sediments and pore waters by accelerated solvent extraction and high performance liquid chromatography-tandem mass spectrometry, Anal. Chim. Acta 872 (2015) 26–34.
[9] Y. Liu, J. Ji, F. Cui, J. Sun, H. Wu, F. Pi, Y. Zhang, X. Sun, Development of a two-step immunochromatographic assay for microcystin-LR based on fluorescent microspheres, Food Contr. 95 (2019) 34–40.
[10] K. Abnous, N.M. Danesh, M.A. Nameghi, M. Ramezani, M. Alibolandi, P. Lavaee, S.M. Taghdisi, An ultrasensitive electrochemical sensing method for detection of microcystin-LR based on infinity-shaped DNA structure using double aptamer and terminal deoxynucleotidyl transferase, Biosens. Bioelectron. 144 (2019) 111674.
[11] Y. Zhao, F. Zheng, W. Ke, W. Zhang, L. Shi, H. Liu, Gap-tethered Au@AgAu Raman tags for the ratiometric detection of MC-LR, Anal. Chem. 91 (2019) 7162–7172.
[12] R. Yang, D. Song, S. Fang, Y. Liu, X. Zhou, F. Long, A. Zhu, Development of novel portable and reusable fiber optical chemiluminescent biosensor and its application for sensitive detection of microcystin-LR, Biosens. Bioelectron. 121 (2018) 27–33.
[13] Z. Wu, D. He, B. Cui, Z. Jin, Ultrasensitive detection of microcystin-LR with gold immunochromatographic assay assisted by a molecular imprinting technique, Food Chem. 283 (2019) 517–521.
[14] M. Zhao, H. Yu, Y. He, A dynamic multichannel colorimetric sensor array for highly effective discrimination of ten explosives, Sens. Actuators B Chem. 283 (2019) 329–333.
[15] L. Zheng, G. Cai, S. Wang, M. Liao, Y. Li, J. Lin, A microfluidic colorimetric biosensor for rapid detection of Escherichia coli O157:H7 using gold nanoparticle aggregation and smart phone imaging, Biosens. Bioelectron. 124–125 (2019) 143–149.
[16] X. Li, R. Cheng, H. Shi, T. Bo, G. Zhao, A simple highly sensitive and selective aptamer-based colorimetric sensor for environmental toxins microcystin-LR in water samples, J. Hazard Mater. 304 (2015) 474–480.
[17] L. Guo, H. Zheng, C. Zhang, L. Qu, L. Yu, A novel molecularly imprinted sensor based on PtCu bimetallic nanoparticle deposited on PSS functionalized graphene with peroxidase-like activity for selective determination of puerarin, Talanta 210 (2020) 120621.
[18] J. Wang, M. Bao, T. Wei, Z. Wang, Z. Dai, Bimetallic metal-organic framework for enzyme immobilization by biomimetic mineralization: constructing a mimic enzyme and simultaneously immobilizing natural enzymes, Anal. Chim. Acta 1098 (2020) 148–154.
[19] L. Gao, J. Zhuang, L. Nie, J. Zhang, Y. Zhang, N. Gu, T. Wang, J. Feng, D. Yang, S. Perrett, X. Yan, Intrinsic peroxidase-like activity of ferromagnetic nanoparticles, Nat. Nanotechnol. 2 (2007) 577–583.
[20] Y. Huang, J. Ren, X. Qu, Nanozymes: classification, catalytic mechanisms, activity regulation, and applications, Chem. Rev. 119 (2019) 4357–4412.
[21] X. Ye, X. He, Y. Lei, J. Tang, Y. Yu, H. Shi, K. Wang, One-pot synthesized Cu/Au/Pt trimetallic nanoparticles with enhanced catalytic and plasmonic properties as a universal platform for biosensing and cancer theranostics, Chem. Commun. 55 (2019) 2321–2324.
[22] P. Wu, P. Ding, X. Ye, L. Li, K. Wang, One-pot synthesized Cu/Au/Pt trimetallic nanoparticles as a novel enzyme mimic for biosensing applications, RSC Adv. 9 (2019) 14982–14989.
[23] S. Nagahara, T. Matsuda, Hydrogel formation via hybridization of oligonucleotides derivatized in water-soluble vinyl polymers, Polym. Gels Netw. 4 (1996) 111–127.
[24] M. Oishi, K. Nakatani, Dynamically programmed switchable DNA hydrogels based on a DNA circuit mechanism, Small 15 (2019) 1900490.
[25] H. Yang, H. Liu, H. Kang, W. Tan, Engineering target-responsive hydrogels based on aptamer-target interactions, J. Am. Chem. Soc. 130 (2008) 6320–6321.
[26] L. Yan, Z. Zhu, Y. Zou, Y. Huang, D. Liu, S. Jia, D. Xu, M. Wu, Y. Zhou, S. Zhou, C.J. Yang, Target-responsive "Sweet" hydrogel with glucometer readout for portable and quantitative detection of non-glucose targets, J. Am. Chem. Soc. 135 (2013) 3748–3751.
[27] Y. Li, Y. Ma, X. Jiao, T. Li, Z. Lv, C.J. Yang, X. Zhang, Y. Wen, Control of capillary behavior through target-responsive hydrogel permeability alteration for sensitive visual quantitative detection, Nat. Commun. 10 (2019) 1036.
[28] S. Deng, J. Yan, F. Wang, Y. Su, X. Zhang, Q. Li, G. Liu, C. Fan, H. Pei, Y. Wan, In

situ terminus-regulated DNA hydrogelation for ultrasensitive on-chip microRNA assay, Biosens. Bioelectron. 137 (2019) 263–270.
[29] Y. He, X. Yang, R. Yuan, Y. Chai, Switchable target-responsive 3D DNA hydrogels as a signal amplification strategy combining with SERS technique for ultrasensitive detection of miRNA 155, Anal. Chem. 89 (2017) 8538–8544.
[30] M. Zhao, P. Wang, Y. Guo, L. Wang, F. Luo, B. Qiu, L. Guo, X. Su, Z. Lin, G. Chen, Detection of aflatoxin B1 in food samples based on target-responsive aptamer-cross-linked hydrogel using a handheld pH meter as readout, Talanta 176 (2018) 34–39.
[31] R. Liu, Y. Huang, Y. Ma, S. Jia, M. Gao, J. Li, H. Zhang, D. Xu, M. Wu, Y. Chen, Z. Zhu, C. Yang, Design and synthesis of target-responsive aptamer-cross-linked hydrogel for visual quantitative detection of ochratoxin A, ACS Appl. Mater. Interfaces 7 (2015) 6982–6990.
[32] J. Li, L. Mo, C.H. Lu, T. Fu, H.H. Yang, W. Tan, Functional nucleic acid-based hydrogels for bioanalytical and biomedical applications, Chem. Soc. Rev. 45 (5) (2016) 1410–1431.
[33] S.M. Taghdisi, N.M. Danesh, M. Ramezani, N. Ghows, S.A. Mousavi Shaegh, K. Abnous, A novel fluorescent aptasensor for ultrasensitive detection of microcystin-LR based on single-walled carbon nanotubes and dapoxyl, Talanta 166 (2017) 187–192.
[34] L. Feng, A. Zhu, H. Wang, H. Shi, A nanosensor based on quantum-dot haptens for rapid, on-site immunoassay of cyanotoxin in environmental water, Biosens. Bioelectron. 53 (2014) 1–4.
[35] K. Zhang, K. Dai, R. Bai, Y. Ma, Y. Deng, D. Li, X. Zhang, R. Hu, Y. Yang, A competitive microcystin-LR immunosensor based on Au NPs@metal-organic framework (MIL-101), Chin. Chem. Lett. 30 (2019) 664–667.
[36] Y. Zhang, M. Chen, H. Li, F. Yan, P. Pang, H. Wang, Z. Wu, W. Yang, A molybdenum disulfide/gold nanorod composite-based electrochemical immunosensor for sensitive and quantitative detection of microcystin-LR in environmental samples, Sens. Actuators B Chem. 244 (2017) 606–615.
[37] W. Zhang, C. Han, B. Jia, C. Saint, M. Nadagouda, P. Falaras, L. Sygellou, V. Vogiazi, D.D. Dionysiou, A 3D graphene-based biosensor as an early microcystin-LR screening tool in sources of drinking water supply, Electrochim. Acta 236 (2017) 319–327.
[38] F. Wang, S. Liu, M. Lin, X. Chen, S. Lin, X. Du, H. Li, H. Ye, B. Qiu, Z. Lin, L. Guo, G. Chen, Colorimetric detection of microcystin-LR based on disassembly of orient-aggregated gold nanoparticle dimers, Biosens. Bioelectron. 68 (2015) 475–480.